COMPARISON OF IONOSPHERIC ELECTRIC CURRENTS AND PLASMA CONVECTION PATTERNS OBSERVED DURING SUBSTORMS

A. Grocott, S.W.H. Cowley and J.A. Davies

Department of Physics and Astronomy, University of Leicester, University Road, Leicester, LE1 7RH, U.K.
Tel: ++44 (0)116 252 3563 Fax: ++44 (0)116 252 3555 Email: A.Grocott@ion.le.ac.uk

Abstract. The effect of magnetospheric substorms on the global ionospheric convection pattern is widely debated. Discussed here, is a study made of ionospheric electric currents, co-incident with plasma convection at the time of substorm onset, using the HF radars of the Super Dual Auroral Radar Network (SuperDARN), and the global array of ground magnetometers. Preliminary results are presented, which utilise an ionospheric potential mapping model to produce plasma convection vectors and electric potential contours, with corresponding ionospheric currents being derived from magnetic perturbations. Clear indications of a relationship between the substorm current system and the plasma convection patterns are seen.

1. Introduction

It is well established that magnetic reconnection at the magnetopause (determined largely by coupling processes between the geomagnetic and interplanetary magnetic fields) results in the modification of the large scale ionospheric flow pattern [*Etemadi et al.,* 1988; *Todd et al.,* 1988]. What is less well established, is how that pattern is modified by corresponding night-side reconnection. *Opgenoorth and Pellinen* [1998] found that the global convection system intensifies in association with substorm onset. In this study, SuperDARN measurements of plasma convection velocities are used, along with ionospheric electric current patterns derived from magnetic data, to further investigate the ionospheric flows associated with substorm onset.

It is necessary to consider two essentially independent components of the flow which are related to the generation and destruction of open field lines [*Cowley and Lockwood,* 1992]. For the purposes of this study, these two components, illustrated in figure 1, can be classified in terms of basic substorm physics. The first component, associated with dayside reconnection is related to the growth phase, and is "directly driven" by the solar wind. The second component, associated with field line dipolarisation and tail reconnection, is related to the expansion and recovery phases and represents the magnetosphere's "unloading" response to that driving [*Cowley et al.,* 1998]. However, in reality both of these components generally occur simultaneously and it is the aim of this study to identify, if possible, those effects on the global ionospheric flow picture which can be attributed to a substorm onset.

2. Experimental Facilities

Two main experimental facilities have been used for the acquisition of data for this study, namely, the SuperDARN HF radar system and a semi-global network of 68 magnetometers. The magnetometer network consists of stations from the IMAGE [*Lühr et al.,* 1998], SAMNET [*Yeoman et al.,* 1990], MACCS [*Hughes and Engebretson,* 1997], CANOPUS [*Grant et al.,* 1992] and Greenland [*Friis-Christensen et al.,* 1988] magnetometer chains. All references to the location of facilities used in the study are given in Altitude Adjusted Corrected Geomagnetic (AACGM) coordinates, a development of the PACE coordinate system discussed by *Baker and Wing* [1989].

SuperDARN is comprised of an auroral network of HF radars in both the northern and southern hemispheres. The northern hemisphere network used in this study consists of eight radars (six of which were operational at the time of the event considered here) (figure 2). This clearly illustrates the ability of SuperDARN to image large-scale high-latitude convection [*Greenwald et al.,* 1995]. In fact, the radars are arranged such that observations are made in common areas and hence the two-dimensional $\mathbf{E}\wedge\mathbf{B}$ velocity can be measured directly. By merging measurements from all the radars in the northern hemisphere, direct mapping of the convection can be extended to almost 12 hours of magnetic local time. However, the two-dimensional velocity at any point can only be unambiguously resolved if backscatter is simultaneously present in the field of view of two radars. This is frequently not the case, and thus the possibilities for the large-scale convection velocity patterns to be derived is very constrained.

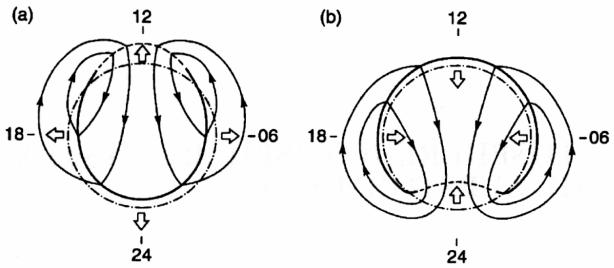

Figure 1. Sketches of the basic components of the ionospheric flow associated with the substorm cycle, for (a) steady unbalanced reconnection at the dayside magnetopause, and (b) steady unbalanced reconnection in the tail [from *Cowley et. al.,* 1998].

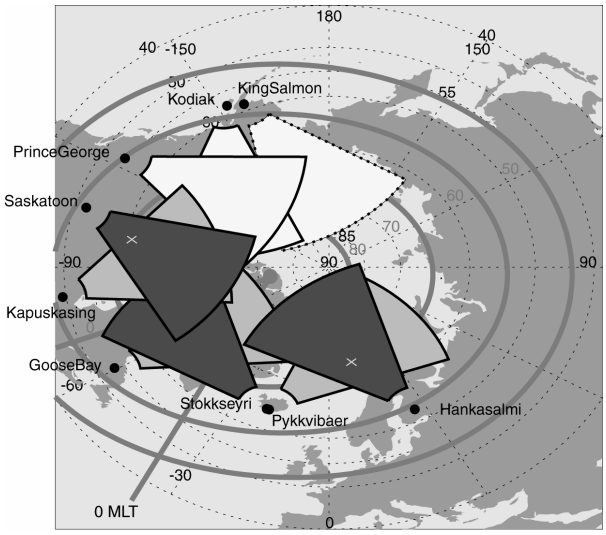

Figure 2. The locations and fields of view of the northern hemisphere SuperDARN HF radars. The three pairs of radars used in this study, have their fields of view shaded grey. The crosses on the Saskatoon and Hankasalmi fields of view indicate the locations of the range gate used for time-series analysis. Magnetic Local Midnight at 02:00 UT is also indicated.

A model developed by *Ruohoniemi and Baker* [1998] attempts to overcome this problem by deriving large-scale global convection maps from the line-of-sight velocities, via mathematical fitting of the data to an expansion of the electrostatic potential in spherical harmonics. The line of sight velocity data are filtered and mapped onto a polar grid and then fitted to the model, enabling the convection pattern that is most consistent with the measurements to be determined. Information from a statistical model is used to stabilise the solution where no measurements are available thus optimising the mapping of large-scale convection patterns. For the purpose of this study, this 'Map Potential' model has been used to produce maps of ionospheric potential contours, which illustrate the plasma flow patterns as well as giving an indication of the cross polar cap potential.

3. Observations

A number of intervals have been chosen for this investigation, which show both well-defined substorm onsets and good coverage by the SuperDARN radars. Data from a typical example are presented here (figure 3) from 00:00 UT on 1 November 1998, when Greenland was near magnetic local midnight. Data from the WIND satellite is shown in panel (a). It should be noted that this data has been shifted by 27 minutes, to account for the time delay between a feature being observed by WIND and it reaching the ionosphere. This delay consists of the sum of three components: (1) the time between the appearance of the feature at the spacecraft and its arrival at the subsolar bowshock, (2) the frozen-in transit time across the subsolar magneto-

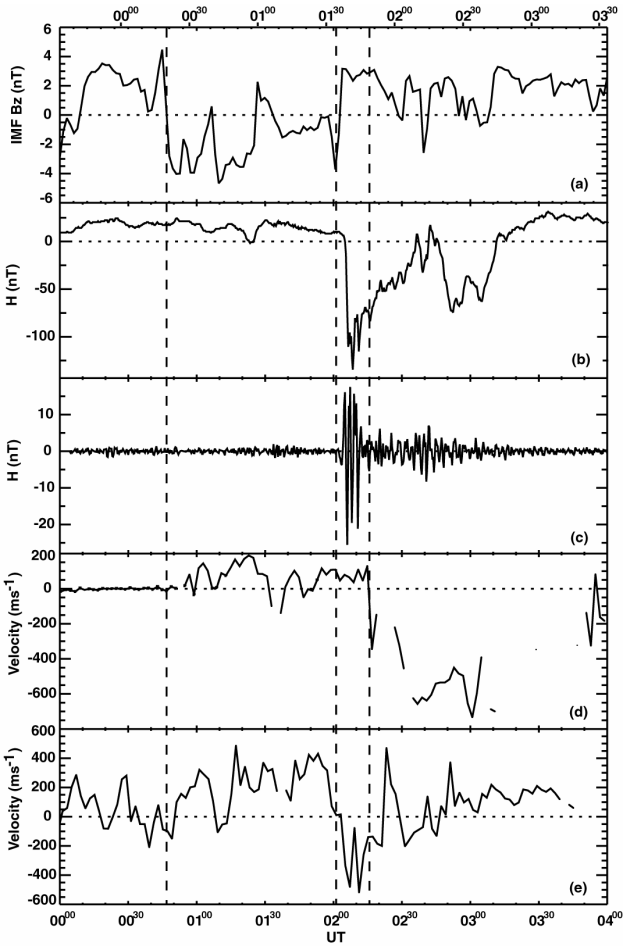

Figure 3. Examples of the various data sets used in this study from 1 November, 1998: (a) IMF Bz data from the WIND spacecraft, shifted by 27 minutes to account for the spacecraft – ionosphere time delay. The axis at the top of this figure, shows the non-shifted time. (b) Shows unfiltered data, and (c) filtered data (20-200s) from the Frederikshab magnetometer. (d) Line of sight velocity data from the Saskatoon and (e) Hankasalmi SuperDARN radars, where positive velocities are towards the radar and negative velocities are away.

sheath, and (3) the Alfvénic propagation time along open field lines from the subsolar magnetopause to the cusp ionosphere [*Khan and Cowley*, 1999]. A southward turning of the IMF is evident in the WIND data at 00:47 UT (shifted time), which then remained predominantly southward until just after 02:00 UT. At this time, a substorm onset is detected at the Frederikshab magnetometer station (68.2°N, 39.7°E) which lied at 23:55 MLT. The data ('H' component) from the Frederikshab magnetometer is presented in panel (b), with filtered data (20-200 seconds), in panel (c), showing a Pi2 signature at 02:02 UT. Panels (d) and (e) contain time series data from the Saskatoon radar (beam 7, range 25, at 72.1°N, -36.2°E) and the Hankasalmi radar (beam 5, range 32, at 72.3°N, 101.8°E) respectively. At the time of substorm onset, Saskatoon was in the dusk cell at 18:50 MLT, and Hankasalmi was in the

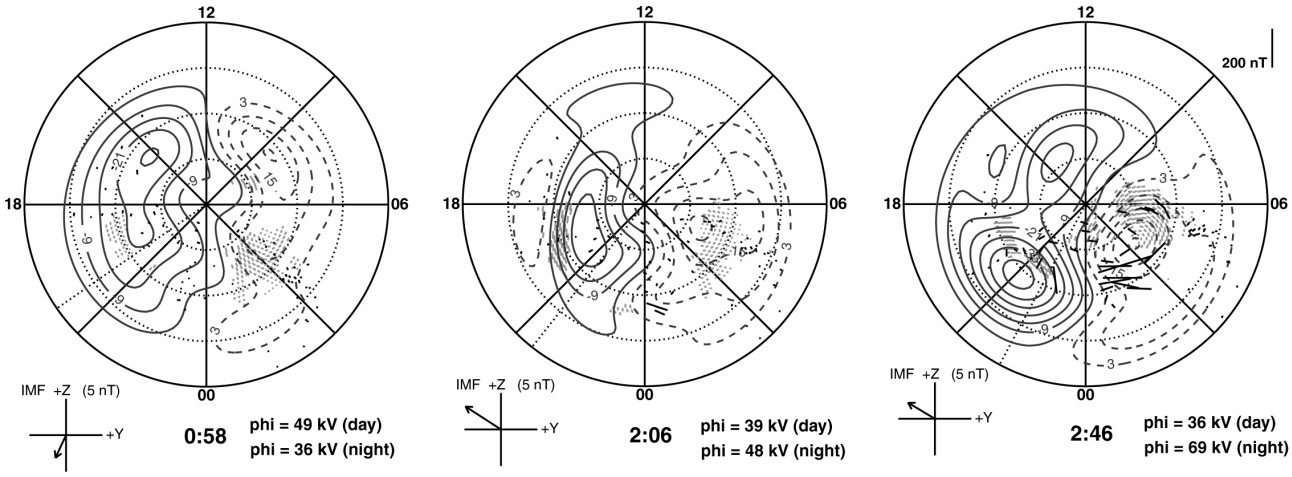

Figure 4. MLT plots illustrating the electric potential contours of the ionospheric flow cells, as derived by the Map Potential Model, overlaid with inverted magnetic perturbations showing **E**∧**B** drift. The shaded areas indicate where radar data is present to influence the model. The concentric circles are marked at 10° of magnetic latitude, from 50° to 90°.

dawn cell at 04:00 MLT. At 00:47 UT, when the period of southward IMF was first detected at the ionosphere, enhanced line of sight flow speeds are clearly seen by Saskatoon, with less obvious but none the less evident enhancements visible in the Hankasalmi data. Then, shortly after substorm onset has been detected at Frederikshab, Hankasalmi sees a noticeable change in the flow again, with Saskatoon registering a sizeable perturbation some 15 minutes later.

4. Analysis

To better visualise the ionospheric Hall currents which give rise to the magnetic perturbations, plots in magnetic local time were produced, of the magnetic data superimposed on the electrostatic potential contours from the map potential model. The fitted radar data are also plotted, to give an indication of data input to the fit. Data from all five magnetometer chains were taken and converted into the same geomagnetic co-ordinate system (using the IGRF where necessary). The data were averaged at a temporal resolution of 2 minutes to correspond to the integration time of the HF radars. It was subsequently rotated anti-clockwise through 90° and plotted as pseudo **E**∧**B** drift vectors, assuming that the main currents are Hall currents. Three examples of these plots are shown in figure 4. The first, at 00:58 UT shows the flow pattern before substorm onset, during the period of southward IMF discussed earlier. Clearly seen in this plot the foci of the two cells lie on the dayside, in agreement with figure 1a for flux input to the system, with a cross-polar cap potential of 49kV. The second plot at 02:06 UT is immediately after substorm onset, evident by the appearance of the sub-storm electrojet just post-midnight. Here the foci of the cells have moved onto the nightside, and although the total cross polar cap potential has not changed significantly (48kV), it is now clearly centred on the nightside sector. In the third plot at 02:46 UT, around the time of maximum extent of the substorm, we can clearly see the situation of figure 1b, where there are considerably enhanced flows on the nightside. The substorm electrojet is now clearly visible, with a definite (but insufficient) eastward curving of the flow in this region, and this is reflected in the large increase in potential difference of 20kV apparent in the nightside ionosphere.

In order to see these changes evolving temporally, the maximum nightside ionospheric potential difference has been determined from the potential contours, and plotted as a time series in figure 5b. These values were determined by taking the difference between the maximum potentials from the dawn and dusk cells that were seen on the nightside. A 10 minute running mean has been applied to the data, to filter out high frequency variations. A pseudo AE index has also been derived (from all 68 magnetometers) to give an indication of the corresponding magnetic activity (figure 5c); also shown is IMF Bz (figure 5a), again shifted by 27 minutes to account for the ionospheric time lag. From figure 5, (which shows data from 20:00 UT on 31 October), several instances of enhanced potential difference can be identified, at 23:30 (on the 31st), 01:20, 02:15, 06:20 and 07:00 UT. All of these enhancements can be accounted for by corresponding periods of negative IMF Bz (indicated in figure 5 by the dashed vertical lines), when the flow would be enhanced by dayside reconnection. However, this still leaves a large flow enhancement feature apparent between 02:30 and 03:45 UT (corresponding to the shaded area in the figure), during which time the peak potential difference occurs. There is no corresponding negative Bz interval and hence the flow must have been excited by some other means. Figure 5b clearly shows this enhancement corresponding to a large value of AE, which is in agreement with our previous deduction that the flow is substorm driven.

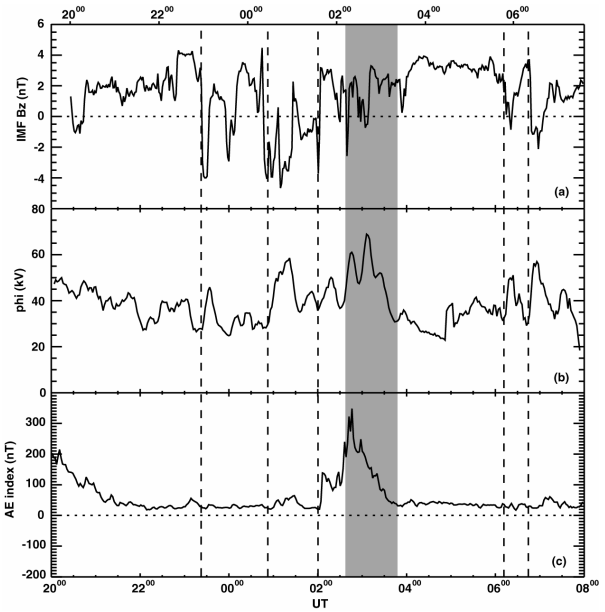

Figure 5. Data from 31 October, 1998, showing (a) IMF Bz from the WIND spacecraft, shifted by 27 minutes to account for the spacecraft – ionosphere time lag. (b) Maximum nightside ionospheric potential derived from the potential map model, with a 5 point running mean. (c) Pseudo AE, derived from the 68 available northern hemisphere magnetometers.

5. Summary

We have used SuperDARN radar data to study the flow response to an isolated substorm, evidenced in ground magnetograms. At the time of substorm onset, the foci of the potential cells migrate towards the nightside, with an increase of more than 20kV in the maximum potential difference between the dawn and dusk cells. From these preliminary results, we can infer a relationship between substorm onset, and the development of nightside enhancements to the ionospheric flow cell patterns. However, before any more definite statements can be made, further investigation is obviously required into a larger sample of events.

Acknowledgements

The authors wish to thank the Finnish Meteorological Institute who maintain the IMAGE magnetometer array, the Canadian Space Agency who constructed and maintain the CANOPUS instrument array, Dr. J. Watermann of the Danish Meteorological Institute for providing the Greenland magnetometer data, and Boston University and Augsburg College, who, with assistance from the University of Alberta and the Geological Survey of Canada, run the MACCS magnetometer array, which is supported by the National Science Foundation's Magnetospheric Physics Program. We also thank Dr I.R. Mann and Dr D.K. Milling for the SAMNET data. SAMNET is a PPARC National Facility deployed and operated by the University of York.

References

Baker, K.B., and S. Wing, A new magnetic coordinate system for conjugate studies at high latitudes, *J. Geophys. Res., 94*, 9139-9143, 1989.

Cowley, S.W.H., H. Kahn, and A. Stockton-Chalk, Plasma flow in the coupled magnetosphere-ionosphere system and its relationship to the substorm cycle, *Proceedings of ICS-4*, edited by S. Kokburn, and Y. Kamide, pp. 623-628, Terra Sci. Pub. Co. / Kluwer Academic Pub., 1998.

Cowley, S.W.H., and M. Lockwood, Excitation and decay of solar wind-driven flows in the magnetosphere-ionosphere system, *Ann. Geophysicae, 10*, 103, 1992.

Etemadi, A., et al., The dependence of high-latitude ionospheric flows on the north-south component of the IMF: A high-time resolution correlation analysis using EISCAT "Polar" and AMPTE-UKS and –IRM data, *Planet. Space Sci., 36*, 471-498, 1988.

Friis-Christensen, E., et al., Ionospheric travelling convection vortices observed near the polar cleft: a triggered response to sudden changes in the solar wind, *Geophys. Res. Lett., 15*, 253, 1988.

Grant, I.F., D.R. McDiarmid, and A.G. McNamara, A class of high-*m* pulsations and its auroral radar signature, *J. Geophys. Res., 97*, 8439-8451, 1992.

Greenwald, R.A., et al., DARN/SuperDARN: A global view of the dynamics of high-latitude convection, *Space Sci. Rev., 71*, 761-796, 1995.

Hughes, W.J., and M.J. Engebretson, MACCS: Magnetometer Array for Cusp and Cleft Studies, in *Satellite-Ground Based Coordination Sourcebook*, edited by M. Lockwood, M.N. Wild, H. J. Opgenoorth, ESA-SP-1198, pp. 119-130, 1997.

Khan, H., and S.W.H. Cowley, Observations of the response time of high-latitude ionospheric convection to variations in the interplanetary magnetic field using EISCAT and IMP-8 data, *Ann. Geophysicae, 17*, 1305-1335, 1999.

Lühr, H., et al., Westward moving dynamic substorm features observed with the IMAGE magnetometer network and other ground-based instruments. *Ann. Geophysicae, 16*, 425-440, 1998.

Opgenoorth, H.J., and R.J. Pellinen, The reaction of the global convection electrojets to the onset and expansion of the substorm current wedge, *Proceedings of ICS-4*, edited by S. Kokburn, and Y. Kamide, pp. 663-668, Terra Sci. Pub. Co. / Kluwer Academic Pub., 1998.

Ruohoniemi, J.M., and K.B. Baker, Large-scale imaging of high-latitude convection with Super Dual Auroral Radar Network HF radar observations, *J. Geophys. Res., 103*, 20,797-20,811, 1998.

Todd, H., et al., Response time of the high-latitude dayside ionosphere to sudden changes in the north-south component of the IMF, *Planet. Space Sci., 36*, 1415-1428, 1988.

Yeoman, T.K., D.K. Milling, and D. Orr, Pi2 pulsation polarisation patterns on the U.K. Sub-auroral Magnetometer Network (SAMNET), *Planet Space Sci., 38*, 589-602, 1990.